Stem Cell Reports
Report
OPEN ACCESS

Tissue-Engineered Vascular Rings from Human iPSC-Derived Smooth Muscle Cells

Biraja C. Dash,[1,2,3] Karen Levi,[4] Jonas Schwan,[5] Jiesi Luo,[1,2] Oscar Bartulos,[1,2] Hongwei Wu,[1,2,6] Caihong Qiu,[2] Ting Yi,[1,2] Yongming Ren,[1,2] Stuart Campbell,[5] Marsha W. Rolle,[4] and Yibing Qyang[1,2,7,8,*]
[1]Section of Cardiovascular Medicine, Department of Internal Medicine, Yale Cardiovascular Research Center, Yale School of Medicine, New Haven, CT 06511, USA
[2]Yale Stem Cell Center, Yale University, New Haven, CT 06510, USA
[3]Department of Surgery (Plastic), Yale University, New Haven, CT 06520, USA
[4]Department of Biomedical Engineering, Worcester Polytechnic Institute, Worcester, MA 01609, USA
[5]Department of Biomedical Engineering, Yale University, New Haven, CT 06510, USA
[6]Department of Orthopedics, Hunan Cancer Hospital and The Affiliated Cancer Hospital of Xiangya School of Medicine, Central South University, Changsha, Hunan 410011, China
[7]Vascular Biology and Therapeutics Program, Yale School of Medicine, New Haven, CT 06510, USA
[8]Department of Pathology, Yale University, New Haven, CT 06510, USA
*Correspondence: yibing.qyang@yale.edu
http://dx.doi.org/10.1016/j.stemcr.2016.05.004

SUMMARY

There is an urgent need for an efficient approach to obtain a large-scale and renewable source of functional human vascular smooth muscle cells (VSMCs) to establish robust, patient-specific tissue model systems for studying the pathogenesis of vascular disease, and for developing novel therapeutic interventions. Here, we have derived a large quantity of highly enriched functional VSMCs from human induced pluripotent stem cells (hiPSC-VSMCs). Furthermore, we have engineered 3D tissue rings from hiPSC-VSMCs using a facile one-step cellular self-assembly approach. The tissue rings are mechanically robust and can be used for vascular tissue engineering and disease modeling of supravalvular aortic stenosis syndrome. Our method may serve as a model system, extendable to study other vascular proliferative diseases for drug screening. Thus, this report describes an exciting platform technology with broad utility for manufacturing cell-based tissues and materials for various biomedical applications.

INTRODUCTION

Dysfunction of vascular smooth muscle cells (VSMCs) frequently leads to vascular disease and represents one of the largest causes of mortality (Michel et al., 2012). Animal models and primary VSMC culture-based approaches have been informative in unraveling disease mechanisms (Chang et al., 2014; Zaragoza et al., 2011). However, there are significant barriers to progress in the field of basic and translational research of vascular disease due to (1) significant differences in vascular physiology between mice and humans; (2) limited access to patient VSMCs; and (3) lack of patient-specific, 3D tissue models that provide a closer approximation of the in vivo environment. It is also worth noting that the lack of robust human cell-based disease models has contributed to the failure of a number of clinical trials that were largely based upon animal studies (Rubin, 2008). Thus, it is necessary to obtain an abundant and renewable source of functional human VSMCs and to establish robust, human tissue model systems for studying the pathogenesis of vascular disease, and for developing novel therapeutic interventions.

Induced pluripotent stem cell (iPSC) technology holds great promise for future autologous cellular therapies for vascular diseases (Tavernier et al., 2013). However, a major concern is the availability of approaches to differentiate iPSCs into large quantities of functional VSMCs for research and therapeutic applications (Dash et al., 2015). VSMCs have been previously derived from human iPSCs (hiPSCs) with different approaches (Bajpai et al., 2012; Cheung et al., 2012; Lee et al., 2009; Patsch et al., 2015; Wanjare et al., 2013). However, an efficient, large-scale production of highly enriched, functional hiPSC-VSMCs suitable for vascular tissue engineering still awaits to be established. In this study, hiPSCs from fibroblast cells were generated using Sendai virus (SeV) vectors. We also derived a large quantity of highly enriched, functional hiPSC-VSMCs based on a robust embryoid body (EB) approach. In addition, we used a scaffold-free, self-assembly approach to engineer robust 3D model vascular tissue constructs from both normal and disease-specific human VSMCs.

RESULTS

Integration-free hiPSC Generation and Characterization

Integration-free hiPSCs were generated with neonatal skin fibroblast cells derived from a healthy female donor using SeV particles that encode OCT3/4, KLF4, SOX2, and c-MYC genes. The selected hiPSC clones exhibited a

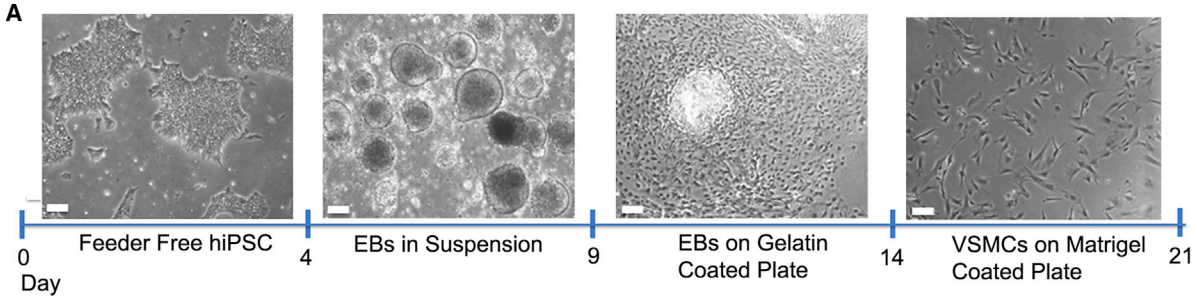

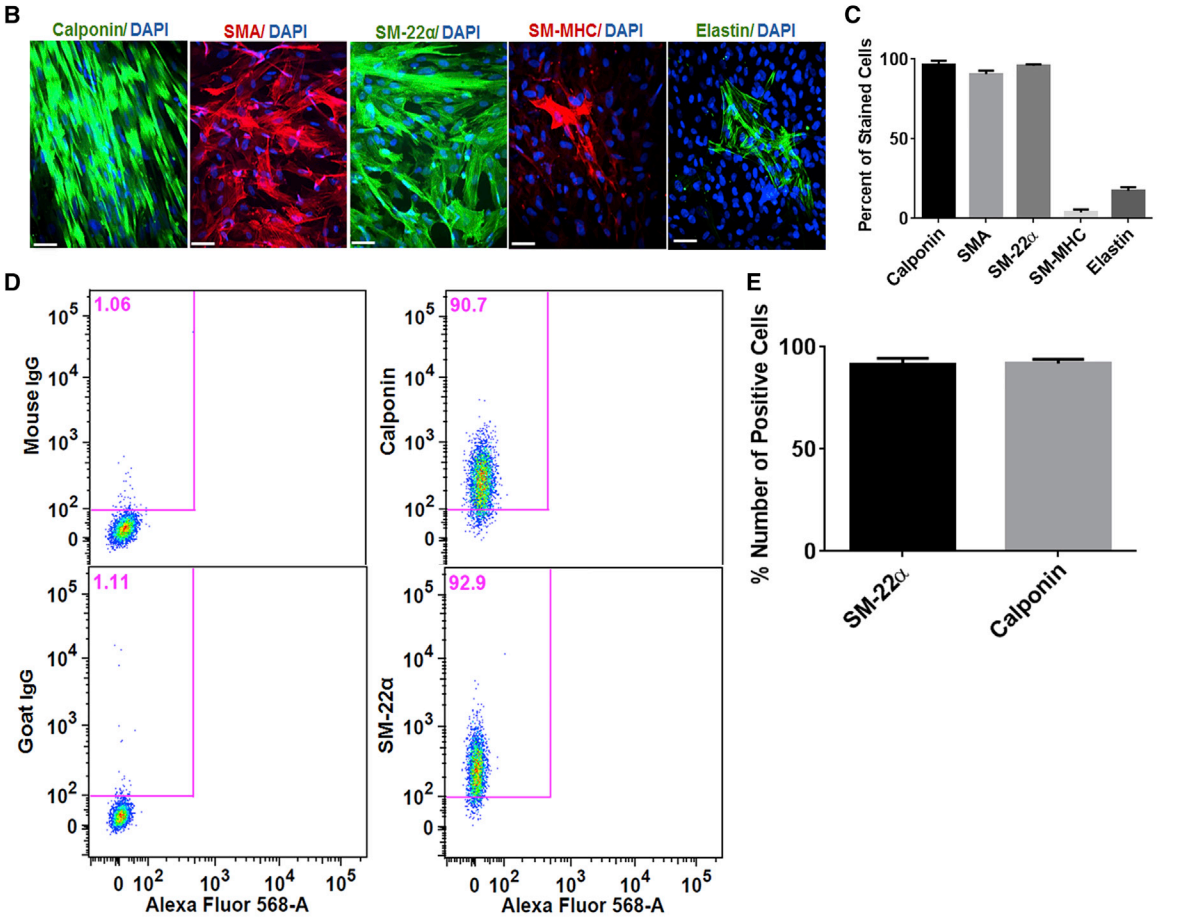

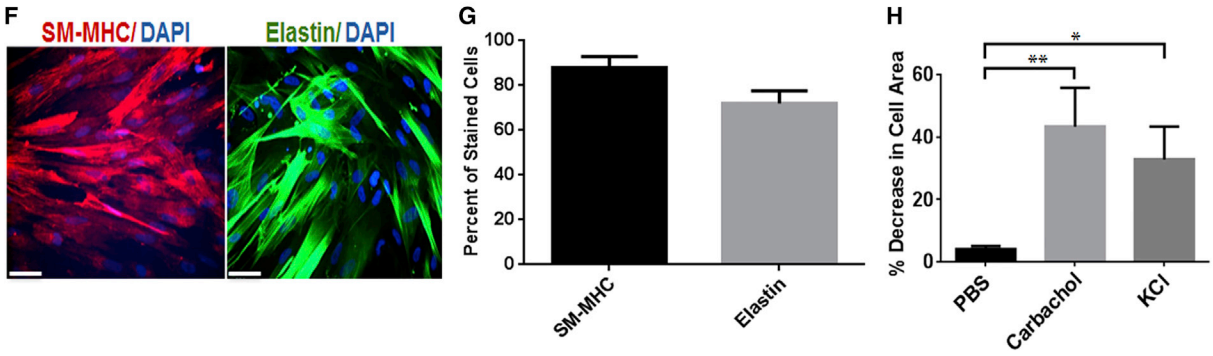

(legend on next page)

typical compact phenotype indistinguishable from human embryonic stem cells and were positive for pluripotency markers, including OCT4, NANOG, SSEA-4, and Tra-1-60 (Figure S1A). G-band staining for karyotype analysis indicated that hiPSC clones were karyotypically normal (Figure S1B) and were also found to be free of SeV vectors (typically after 15 passages), as shown by RT-PCR (Figure S1C). The hiPSCs formed teratomas and revealed the presence of representative tissues that originated from the three embryonic germ layers (Figure S1D), including the gastrointestinal epithelium (endoderm), pigmented epithelium (ectoderm), and hyaline cartilage (mesoderm). Integration-free hiPSC clones (named as Y6) were then continuously propagated and used for differentiation and characterization of VSMCs.

Derivation of Large Quantities of Pure, Functional VSMCs from hiPSCs

An EB differentiation protocol was used to induce hiPSC differentiation toward a VSMC lineage. The entire differentiation procedure (shown schematically in Figure 1A) requires 21 days starting from hiPSC culture. Since the derivation of VSMCs from hiPSCs using the earlier reported EB method (Xie et al., 2007) was inefficient and could not generate large numbers of VSMCs for therapeutic studies, significant modifications were made to the existing approach, where 80% confluent hiPSCs grown under feeder-free culture were used to make EBs. Moreover, pure mTeSR1 (iPSC self-renewal media) and 25% mTeSR1-containing EB differentiation media was used to culture day 1 and day 2 EBs, respectively. These two modifications resulted in the production of much healthier EBs and an abundance of highly enriched VSMCs. After 7 days of culture in SmGM-2 (a commercially available medium optimized for VSMC growth), 96.25% ± 2.70%, 90.59% ± 2.20%, and 95.81% ± 0.99% of VSMCs expressed calponin, α-smooth muscle actin (SMA), and SM-22α, respectively (Figures 1B, 1C, and S2A). In addition, fluorescence-activated cell sorting (FACS) analysis showed 91.66% ± 2.78% of hiPSC-VSMCs positive for SM-22α and 91.86% ± 2.05% of hiPSC-VSMCs positive for calponin (Figures 1D, 1E, and S2B). The expression of mature VSMC markers such as smooth muscle myosin heavy chain (SM-MHC) and elastin in hiPSC-VSMCs increased from 3.86% ± 1.80% and 17.32% ± 2.30%, when cultured in the SmGM-2 growth medium (Figures 1B and 1C), to 87.45% ± 7.10% and 74.65% ± 4.60%, respectively, when switched to a maturation medium containing 0.5% fetal bovine serum (FBS) and 1 ng/ml transforming growth factor β1 (TGF-β1) for 10 days (Figures 1F and 1G). The expression level of the VSMC mature markers elastin and SM-MHC in the maturation medium was further validated by examining the gene-expression level of elastin and by FACS analysis of SM-MHC-positive cells (Figures S2C and S2D). A similar pattern of increase in elastin and SM-MHC was seen after culturing VSMCs in the maturation medium. The elastin gene-expression level increased 3-fold in the maturation medium compared with that in the growth-promoting SmGM-2 medium (Figure S2C). Likewise, an increase in the SM-MHC-positive cells was seen when the VSMCs were cultured in the maturation medium. The SM-MHC-positive cells increased from 3.24% ± 2.76% in SmGM-2 medium to 79.07% ± 5.89% in the maturation medium (Figure S2D). In addition, hiPSC-VSMCs showed contractility in response to agonists such as carbachol and KCl, measured by quantifying percent decrease in the cell area. The treatments with carbachol and KCl induced a 43.31% ± 12.43% and 32.83% ± 10.47% decrease in the cell area, respectively, compared with PBS control (Figures 1H and S3).

The scalability (Figure 2A) and efficiency of the protocol were tested in three different hiPSC lines (all from healthy

Figure 1. Characterization of hiPSC-VSMCs

(A) Schematic diagram along with representative images showing the hiPSC-VSMC differentiation method. Scale bar represents 100 μm.

(B) Immunofluorescence images of cells stained with smooth muscle cell markers calponin, SMA, SM-22α, SM-MHC, and elastin in hiPSC-VSMCs cultured in SmGM-2 medium for 7 days. Red (SMA and SM-MHC), green (SM-22α, calponin, and elastin), and blue (nuclei). Scale bar represents 50 μm. The Y6 hiPSC line was used to derive VSMCs.

(C) Graph showing percentage of VSMCs positive for calponin, SMA, SM-22α, SM-MHC, and elastin in three independent experiments (mean ± SD; n = 3 independent experiments).

(D) Fluorescence-activated cell sorting (FACS) data showing VSMC purity, quantified with smooth muscle cell-specific markers SM-22α and calponin. Goat and mouse IgGs were used as negative controls for SM-22α and calponin, respectively.

(E) Graph showing percentage of VSMCs positive for SM-22α and calponin in three independent FACS experiments (mean ± SD; n = 3 independent experiments).

(F) Immunofluorescence images of hiPSC-VSMCs cultured in a medium containing 0.5% FBS and 1 ng/ml TGF-β1 for 10 days and stained for SM-MHC and elastin. Red (SM-MHC), green (elastin), and blue (nuclei). Scale bar represents 50 μm.

(G) Graph showing percentage of VSMCs positive for SM-MHC and elastin in three independent experiments.

(H) Graph showing percent decrease in cell area in response to agonists KCl and carbachol. Unpaired Student's t test was performed to determine the statistical difference between different groups (mean ± SD; n = 3 independent experiments, *p < 0.05, **p < 0.01). See Figures S1–S3 and Tables S1 and S2 for additional controls and supporting information.

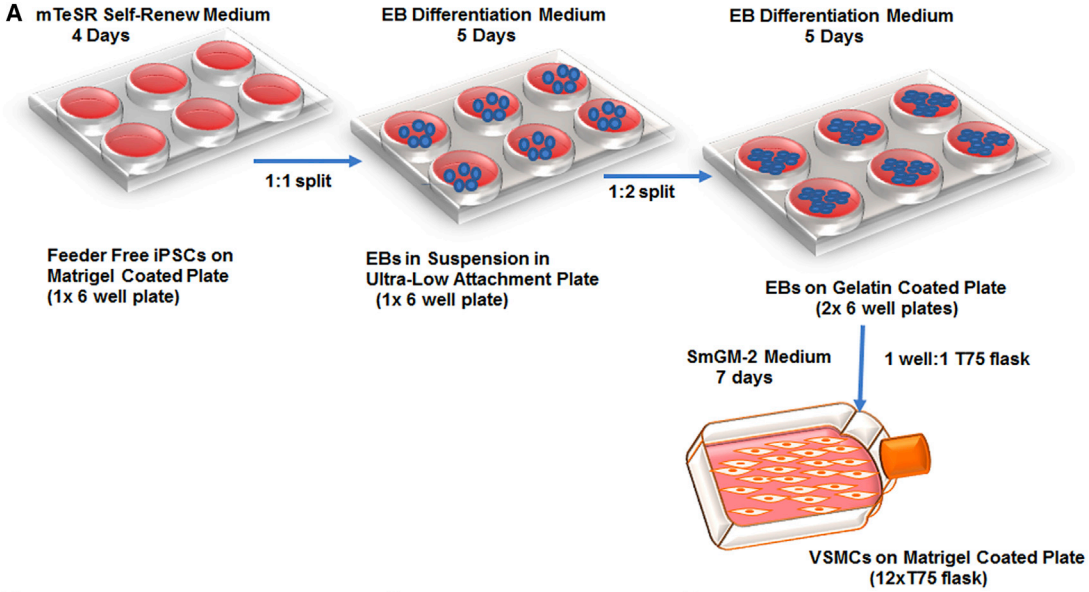

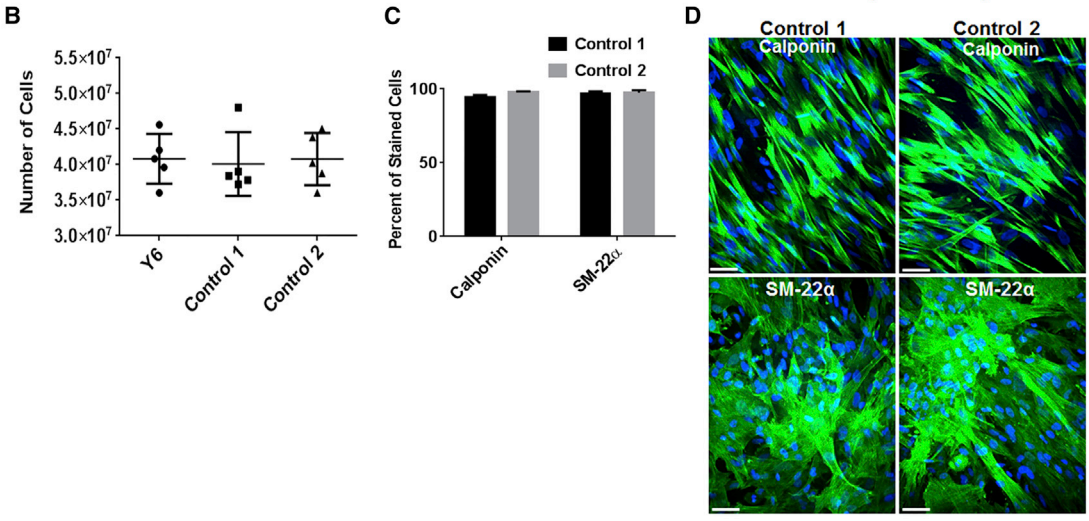

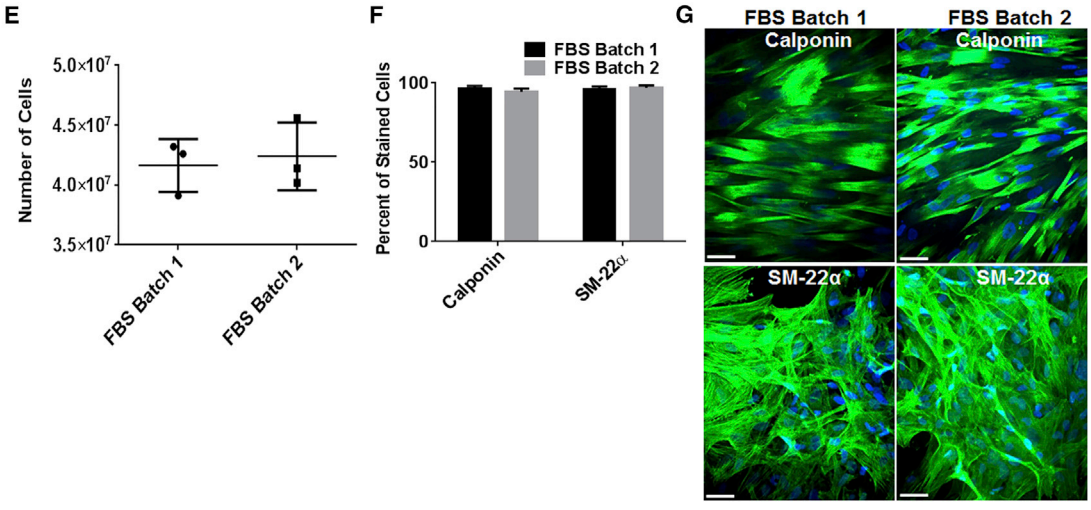

(legend on next page)

subjects): Y6 (established in this study; Figure S1), control 1 (Ge et al., 2012), and control 2 (Chen et al., 2013), and two different batches of FBS (Figures 2B and 2E). The protocol consistently generated about 40 × 10^6 hiPSC-VSMCs for all three hiPSC lines and both batches of FBS (Figures 2B and 2E). In addition, purities of these hiPSC-VSMCs were quantified using SM-22α and calponin. Control 1 and control 2 hiPSC-VSMCs were 94.46% ± 1.30% and 97.96% ± 0.40% positive for calponin and 96.85% ± 1.50% and 97.57% ± 1.50% for SM-22α, respectively (Figures 2C and 2D). Similarly, FBS batch 1- and 2-derived hiPSC-VSMCs were 96.27% ± 1.90% and 94.36% ± 2.00% positive for calponin and 96.11% ± 1.7% and 96.93% ± 1.4% positive for SM-22α, respectively (Figures 2F and 2G).

VSMCs from different vessels have different embryological origin, and these different VSMC subtypes can be distinguished by their distinct in vitro proliferative responses to angiotensin II, TGF-β1, and serum (Cheung et al., 2012). Cell-proliferation assays were performed to determine the hiPSC-VSMC subtype (Figures S2E–S2G). MTT assay after 3 days in culture showed an increased response of hiPSC-VSMCs to serum (Figure S2E), but not to TGF-β1 and angiotensin II. A similar response of hiPSC-VSMCs to serum was observed with cell counting (Figure S2F) and cell-cycle analysis (percentage of proliferating cells in S and G2-M) (Figure S2G). These results are consistent with the notion that hiPSC-VSMCs may contain a significant population of lateral plate mesoderm-derived VSMCs that show a proliferative response to serum but not to TGF-β1 or angiotensin II.

We also found that hiPSC-VSMCs cultured for 7 days in a ring tissue culture medium with 20% FBS, growth factors (platelet-derived growth factor-BB [PDGF-BB] and TGF-β1), and other supplements ($CuSO_4$, proline, glycine, alanine, and ascorbic acid) proliferated (Figure S4A) and were able to produce extracellular matrix such as type I collagen (Figure S4B). This ring culture medium was subsequently used to culture 3D hiPSC-VSMC tissue ring constructs as described below.

Robust Tissue Ring Fabrication and Disease Modeling

Previous studies have reported the use of VSMCs derived from hiPSCs as 2D cell culture models to study vascular disease mechanisms (Ge et al., 2012). However, 3D engineered tissue models may more closely mimic in vivo vascular physiology, as cell-cell and cell-matrix interactions are markedly different between the in vivo environment and in vitro 2D cell culture. So far, only a few studies have reported using stem cell-derived VSMCs for tissue engineering applications using natural or synthetic scaffold materials (Bajpai et al., 2012; Karamariti et al., 2013; Sundaram et al., 2014; Wang et al., 2014). However, none have reported using a scaffold-free approach to create 3D engineered vascular tissues. In this study, we employed a scaffold-free cellular self-assembly approach (Gwyther et al., 2011b) to generate hiPSC-VSMC tissue rings. Briefly, hiPSC-VSMCs cultured in SmGM-2 were harvested and seeded into ring-shaped agarose wells (Figure 3A). hiPSC-VSMCs aggregated and contracted around the center posts of the non-adhesive agarose wells and successfully formed tissue rings within 1 day of seeding.

In preliminary studies, we found that hiPSC-VSMC rings cultured in SmGM-2 continued to contract in the agarose wells, resulting in thinning and failure between 4 and 7 days of culture (Figure S4C). Subsequently, hiPSC-VSMCs were seeded in SmGM-2, then switched to a ring culture medium with 20% FBS, PDGF-BB, TGF-β1, and other collagen-promoting supplements 24 hr after cell seeding. The rings cultured in ring culture medium were stable and did not show appreciable contraction. hiPSC-VSMC rings were cultivated in the ring culture medium for 14–17 days before harvesting for histology and mechanical testing. Representative photographs of tissue rings derived from Y6 hiPSC-VSMCs after 14 days in culture are shown in Figure 3A. Hematoxylin and eosin staining showed highly cellularized tissue rings (Figure 3B). Masson's trichrome staining showed an abundance of collagen in the extracellular matrix of these tissue rings (Figure 3B), which was also shown by immunostaining for type I collagen (Figure S4D). Immunohistochemical analyses also showed

Figure 2. Larger-Scale VSMC Derivation from hiPSCs

(A) Schematic diagram showing the procedure for derivation of hiPSC-VSMCs with high purity.

(B–D) Characterization of hiPSC-VSMCs derived from two other hiPSC lines, control 1 and control 2. Control 1 and control 2 hiPSC-VSMC purity was quantified using calponin and SM-22α markers. (B) Resulting cell numbers from replicate derivations of VSMCs from Y6, control 1, and control 2 hiPSCs after 17 days of differentiation (n = 3 independent experiments). (C) Graph showing percentage of VSMCs positive for calponin or SM-22α in three independent experiments. (D) Representative immunofluorescence images of cells stained with calponin and SM-22α. Green stains for both calponin and SM-22. Blue stains for nuclei. Scale bar represents 50 μm.

(E–G) Characterization of Y6-VSMCs derived using two different batches of FBS. (E) Quantification of cell numbers generated from hiPSC-VSMC derivations using two different batches of serum (n = 3 independent experiments). (F) Graph showing percentage of positive VSMCs for calponin and SM-22α in three independent experiments. (G) Immunofluorescence images of cells stained with calponin and SM-22α. Green stains for both calponin and SM-22α. Blue stains for nuclei. Scale bar represents 50 μm. The data are represented as means ± SD. Also see Figure S2.

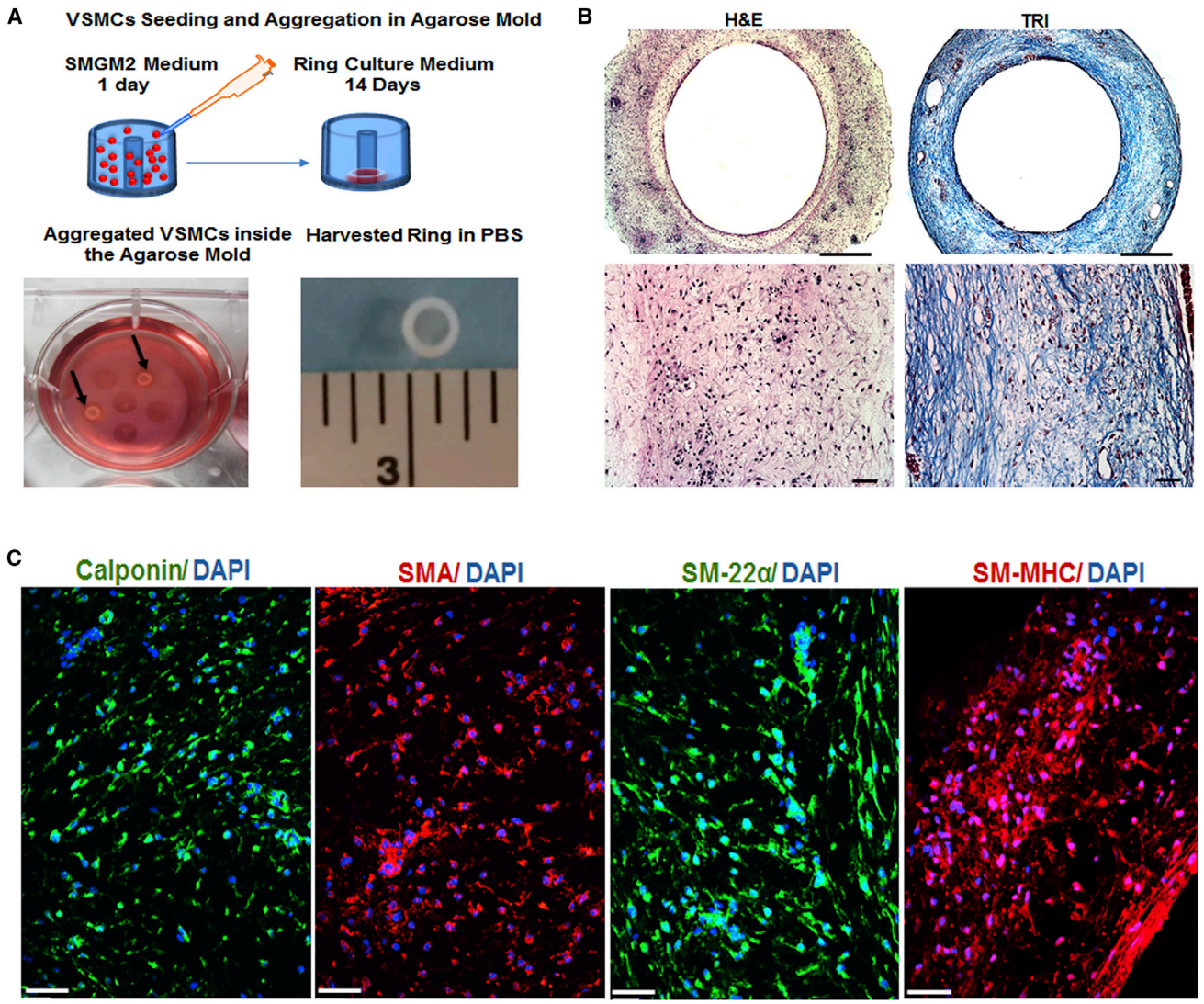

Figure 3. Tissue Ring Fabrication and Characterization Using Y6 hiPSC-VSMCs

(A) Schematic showing tissue ring fabrication by cellular self-assembly, and photographs of tissue rings in the agarose mold (black arrow) and a harvested tissue ring.

(B) Histochemical analysis of the tissue rings with H&E (left) and Masson's trichrome (TRI: right) staining. The pink in H&E staining represents cytoplasm and the blue in Masson's trichrome represents collagen. The dark purple in both H&E and Masson's trichrome staining represents nuclei. Scale bars represent 500 and 100 μm, respectively, for lower and higher magnification images.

(C) Immunofluorescence analysis of calponin (green), SMA (red), SM-22α (green), and SM-MHC (red) present in the tissue rings after 14 days in culture. Blue stains for nuclei. Scale bar represents 50 μm. Also see Figure S4.

that hiPSC-VSMCs within tissue rings cultured for 14 days were positive for calponin, SMA, SM-22α, and SM-MHC (Figure 3C), suggesting that the cells retained a VSMC phenotype during culture as self-assembled, high-density VSMC tissue rings.

Tissue rings from two independent batches were mechanically strong when harvested after 14 or 17 days in culture (Figure 4). Stress-strain plots were generated from each of the tissue ring samples tested (representative plot shown in Figure 4A) and used to calculate ultimate tensile strength (UTS) and maximum tangent modulus. Mechanical testing data for both batches of Y6 hiPSC-VSMC rings are summarized in Figure 4B. The average thickness of the 2 mm inner diameter tissue rings was 0.84–0.87 mm after 14–17 days in culture. Overall, hiPSC-VSMCs exhibited greater UTS than 14-day-old rat aortic or human coronary artery SMC rings (2 mm, inner diameter) reported previously (Gwyther et al., 2011a, 2011b). In addition, the contractile response

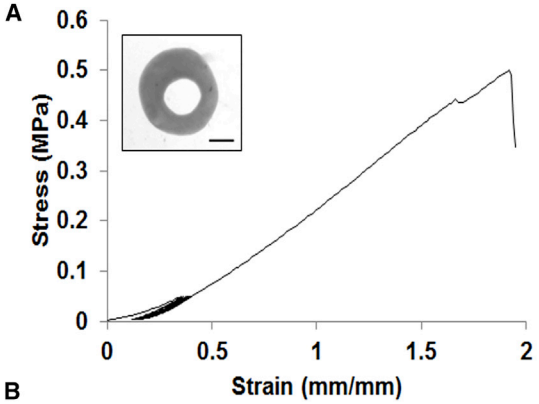

B

Sample Size (n =)	Culture Duration (days)	Ring Thickness (mm)	UTS (MPa)	MTM (MPa)	Max Load (N)	Max Extension (mm)
7	14	0.87 ± 0.05	0.473 ± 0.134	0.442 ± 0.156	0.555 ± 0.140	2.49 ± 0.47
3	17	0.84 ± 0.08	0.366 ± 0.066	0.138 ± 0.021	0.412 ± 0.121	5.84 ± 1.41

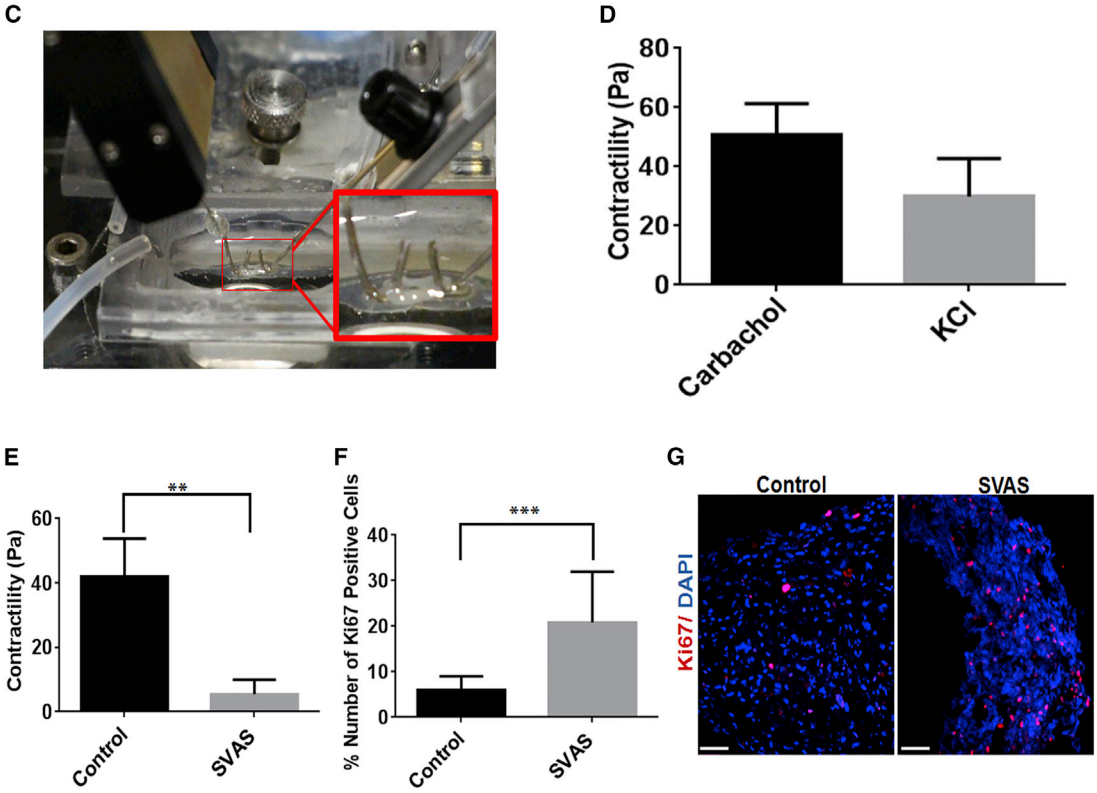

Figure 4. Mechanical and Functional Characterization of hiPSC-VSMC Rings

(A) Representative stress-strain curve of a 14-day-old tissue ring (inset, digital image of ring used to measure thickness and calculate cross-sectional area; scale = 1 mm).

(B) Results of mechanical tests from two independent batches of hiPSC-VSMC tissue rings (mean ± SD; n = 7 and 3 independent measurements for day 14 and 17, respectively).

(legend continued on next page)

of the hiPSC-VSMC tissue rings in response to agonists, carbachol (1 mM) and KCl (50 mM), was measured (Figures 4C and 4D). The contractility was measured using an instrument with a force transducer, in which a contraction by the rings in response to agonists induces an increase in force (Figure 4C). The contraction was shown as tension (Pascal) by a normalizing force with their respective cross-section areas. The rings showed a contraction of 67.35 ± 22.7 Pa in response to carbachol, whereas the response was 44.44 ± 27.13 Pa for KCl (Figure 4D).

Furthermore, we tested whether the tissue ring system could be used to model vascular proliferative diseases such as supravalvular aortic stenosis (SVAS) syndrome. In SVAS, hyperproliferation of VSMCs leads to blockage of the aorta and arteries. Highly enriched VSMCs were derived from control and SVAS (Ge et al., 2012) hiPSCs (Figure S4E). Tissue rings were successfully fabricated from these hiPSC-VSMCs. The tissue rings were characterized for their difference in contractility and percent of proliferating cells using Ki67 immunostaining. The ring contractility study showed control rings with a contraction of 42.01 ± 11.77 Pa in response to carbachol, whereas the response was 5.51 ± 4.51 Pa for SVAS rings (Figure 4E). The percentage of Ki67-positive cells was 6.31% ± 3.16% for control rings and 21.73% ± 11.96% for SVAS rings (Figures 4F and 4G). Immunofluorescence analyses of cultured cells revealed more actin filament bundle formation in the control iPSC-VSMCs than in the SVAS iPSC-VSMCs (Figure S4E), consistent with the results described in our earlier report (Ge et al., 2012). In addition, there was an increased percentage of cells expressing SM-MHC in the control iPSC-VSMCs compared with the SVAS iPSC-VSMCs (Figure S4E).

DISCUSSION

In this study, we generated an abundant and renewable source of functional VSMCs from multiple hiPSC lines. The success of VSMC production appears to be independent of the somatic cell sources (Y6: fibroblasts; control 1, VSMCs; control 2, peripheral blood mononuclear cells) and derivation approaches (Y6 and control 2, non-integrating SeV; control 1, lentiviral) used to generate the hiPSC lines. The feeder-free culture approach resulted in healthier and robust EBs, enabling us to derive ~40 million VSMCs within 21 days of differentiation time from a 6-well plate of hiPSCs. The VSMCs were highly enriched for SM-22α, SMA, and calponin and can further be induced into mature VSMCs expressing SM-MHC and elastin. The VSMC derivation method was found to be efficient with different hiPSC lines and also with different batches of FBS. The hiPSC-VSMCs were functional and responded to chemical stimuli such as carbachol and KCl. We have also investigated different VSMC subtypes using an assay described previously (Cheung et al., 2012). hiPSC-VSMCs showed significant proliferation in response to serum, but only exhibited a modest trend of response upon treatment with TGF-β1 or angiotensin II without reaching statistical significance. These results suggest that hiPSC-VSMCs derived in this study may contain a significant population of VSMCs derived from the lateral plate mesoderm.

We then used a cellular self-assembly approach to create hiPSC-VSMC tissue rings. Histological analysis of 14-day-old rings showed high cellularity and VSMC marker expression, including SMA, SM-22α, calponin, and SM-MHC. Type I collagen was also abundantly found in these tissue rings. hiPSC-VSMC tissue rings are mechanically strong enough to endure physical handling and mechanical testing within 7–14 days of cell seeding. In addition, we measured normal and SVAS hiPSC-VSMC contractility in 3D tissue constructs, suggesting that the ring self-assembly system, coupled with patient-specific VSMCs, can be used to create functional model human vascular tissues. SVAS, an autosomal disease, is caused by loss-of-function mutations in the elastin gene and is characterized by hyperproliferation of VSMCs leading to blockage of the ascending aorta and other arterial vessels (Ge et al., 2012). Patients with Williams-Beuren syndrome (WBS) also display SVAS (Ge et al., 2012). Earlier 2D studies in cell culture (Ge et al., 2012; Kinnear et al., 2013) reveal that SVAS and WBS iPSC-VSMCs are less contractile and more proliferative than control iPSC-VSMCs. We were able to model these two important

(C) Photograph showing VSMC tissue ring hooked on two micromanipulators and immersed in a temperature-controlled perfusion bath containing Tyrode's solution for the contractility assay.

(D) Graph showing change in contractility (Pascal) in response to the agonists KCl and carbachol. PBS was used as negative control.

(E) Graph showing change in contractility (Pascal) of control and SVAS rings in response to carbachol. Unpaired Student's t test was performed to determine statistical difference between different groups (mean ± SD; n = 3 independent experiments, $^{**}p < 0.01$). PBS was used as negative control.

(F) Graph showing percent number of Ki67-positive cells in control and SVAS rings. The data are represented as mean ± SD. Unpaired Student's t test was performed to determine statistical difference between different groups (n = 3 independent experiments, $^{***}p < 0.001$).

(G) Representative immunofluorescence images of control and SVAS rings stained with Ki67. Red (Ki67) and blue (nuclei). Scale bar represents 50 μm. Also see Figure S4.

characteristics of SVAS in the physiologically more relevant 3D tissue rings. The SVAS tissue rings showed significantly less contractility and more proliferative cells than control rings. The lower contractile forces generated by SVAS rings might be due to decreased formation of actin filament bundles and fewer cells expressing SM-MHC in SVAS VSMCs compared with those in control VSMCs.

Primary tissue- or hiPSC-derived VSMCs have been previously used to establish vascular tissue constructs with different scaffold materials, such as polyglycolic acid, fibrin, and poly-L-lactic acid (Bajpai et al., 2012; Niklason et al., 1999; Sundaram et al., 2014; Wang et al., 2010). However, these artificial materials are significantly different from the natural extracellular matrix produced by VSMCs. In contrast, our unique scaffold-free technique has enabled fabrication of patient-specific tissue constructs engineered entirely from human VSMCs and the extracellular matrix they produce. The facile, one-step cell-seeding process results in robust, scaffold-free tissue constructs within a short duration of culture time (less than 2 weeks) without specialized equipment. Finally, these tissue rings may be useful as modular building blocks to generate tubular tissue constructs to be used for vascular grafts (Gwyther et al., 2011a, 2011b), or as model in vitro vascular tissues for drug discovery and to study human disease mechanisms.

In the future, we will fabricate tissue rings from various lineage-specific hiPSC-VSMCs and disease-specific VSMCs for disease modeling and drug screening. Further optimization of the culture conditions such as use of Ficoll, a macromolecular crowder, in the culture medium will be tested in order to enhance the strength of the tissue rings (Zeiger et al., 2012). Finally, our methodology can potentially be extended to fabricate tissue rings from other types of cells derived from patient-specific hiPSCs for the construction of mechanically robust engineered tissues for disease research and treatment.

EXPERIMENTAL PROCEDURES

Animal Studies

Immunodeficient Rag2-/-GammaC-/- mice were used for teratoma assay. All animal studies were approved by the Yale IACUC protocol (2013-11347) and performed in accordance with the NIH guidelines for care and use of laboratory animals.

hiPSC-VSMC Derivation

hiPSC-VSMCs were derived using a modified EB protocol which results in a larger-scale generation of VSMCs at the end of 21 days. A detailed protocol is described in the Supplemental Information.

Tissue Ring Fabrication

Custom agarose molds for tissue ring formation were made as previously described (Gwyther et al., 2011a, 2011b), with minor modifications (Dikina et al., 2015). A detailed protocol is described in the Supplemental Information.

2D and 3D Contractility Study

The 2D SMC contraction study was carried out using hiPSC-VSMCs cultured on tissue culture plastic. KCl (50 mM) and carbachol (1 mM) were used as agonists. Similarly, tissue rings were tested for their contractility in response to carbachol. A detailed protocol can be found in the Supplemental Information.

Tissue Ring Mechanical Testing

Mechanical testing was performed using an uniaxial tensile testing machine (Electropuls E1000, Instron) as previously described (Gwyther et al., 2011b). A detailed protocol can be found in the Supplemental Information.

Statistical Analysis

Statistical analyses were performed using GraphPad Prism 6. One-way ANOVA was used to compare the cell proliferation between different time points, and two-tailed Student's t test was used for pair comparisons.

SUPPLEMENTAL INFORMATION

Supplemental Information includes Supplemental Experimental Procedures, four figures, and two tables and can be found with this article online at http://dx.doi.org/10.1016/j.stemcr.2016.05.004.

AUTHOR CONTRIBUTIONS

B.C.D., M.R., and Y.Q. conceived the study; B.C.D., K.L., J.S., O.B., J.L., H.W., C.Q., and T.Y. performed the research; Y.R. and S.C. contributed analytic tools; B.C.D., K.L., J.S., O.B., C.Q., T.Y., M.R., and Y.Q. analyzed the data; B.C.D. and Y.Q. wrote the manuscript; and K.L. and M.R. edited the manuscript.

ACKNOWLEDGMENTS

We would like to thank Drs Laura Niklason and Liqiong Gui for their timely scientific suggestions and Dr Daniel Greif for his suggestions on the manuscript. This work is supported by NSF DGE-1144804 (K.L. and M.R.), NIH 1K02HL101990-01, 1R01HL116705-01, Connecticut's Regenerative Medicine Research Fund (R.M.R.F.) and 12-SCB-YALE-06 (Y.Q.). Control 2 human iPSC line is a generous gift of Dr I-Ping Chen from the University of Connecticut Health Science Center.

Received: March 4, 2015
Revised: May 8, 2016
Accepted: May 8, 2016
Published: July 12, 2016

REFERENCES

Bajpai, V.K., Mistriotis, P., Loh, Y.H., Daley, G.Q., and Andreadis, S.T. (2012). Functional vascular smooth muscle cells derived from human induced pluripotent stem cells via mesenchymal stem cell intermediates. Cardiovasc. Res. *96*, 391–400.

Chang, S., Song, S., Lee, J., Yoon, J., Park, J., Choi, S., Park, J.K., Choi, K., and Choi, C. (2014). Phenotypic modulation of primary vascular smooth muscle cells by short-term culture on micropatterned substrate. PLoS One *9*, e88089.

Chen, I.P., Fukuda, K., Fusaki, N., Iida, A., Hasegawa, M., Lichtler, A., and Reichenberger, E.J. (2013). Induced pluripotent stem cell reprogramming by integration-free Sendai virus vectors from peripheral blood of patients with craniometaphyseal dysplasia. Cell Reprogram. *15*, 503–513.

Cheung, C., Bernardo, A.S., Trotter, M.W., Pedersen, R.A., and Sinha, S. (2012). Generation of human vascular smooth muscle subtypes provides insight into embryological origin-dependent disease susceptibility. Nat. Biotechnol. *30*, 165–173.

Dash, B.C., Jiang, Z., Suh, C., and Qyang, Y. (2015). Induced pluripotent stem cell-derived vascular smooth muscle cells: methods and application. Biochem. J. *465*, 185–194.

Dikina, A.D., Strobel, H.A., Lai, B.P., Rolle, M.W., and Alsberg, E. (2015). Engineered cartilaginous tubes for tracheal tissue replacement via self-assembly and fusion of human mesenchymal stem cell constructs. Biomaterials *52*, 452–462.

Ge, X., Ren, Y., Bartulos, O., Lee, M.Y., Yue, Z., Kim, K.Y., Li, W., Amos, P.J., Bozkulak, E.C., Iyer, A., et al. (2012). Modeling supravalvular aortic stenosis syndrome with human induced pluripotent stem cells. Circulation *126*, 1695–1704.

Gwyther, T.A., Hu, J.Z., Billiar, K.L., and Rolle, M.W. (2011a). Directed cellular self-assembly to fabricate cell-derived tissue rings for biomechanical analysis and tissue engineering. J. Vis. Exp., e3366.

Gwyther, T.A., Hu, J.Z., Christakis, A.G., Skorinko, J.K., Shaw, S.M., Billiar, K.L., and Rolle, M.W. (2011b). Engineered vascular tissue fabricated from aggregated smooth muscle cells. Cells Tissues Organs *194*, 13–24.

Karamariti, E., Margariti, A., Winkler, B., Wang, X., Hong, X., Baban, D., Ragoussis, J., Huang, Y., Han, J.D., Wong, M.M., et al. (2013). Smooth muscle cells differentiated from reprogrammed embryonic lung fibroblasts through DKK3 signaling are potent for tissue engineering of vascular grafts. Circ. Res. *112*, 1433–1443.

Kinnear, C., Chang, W.Y., Khattak, S., Hinek, A., Thompson, T., de Carvalho Rodrigues, D., Kennedy, K., Mahmut, N., Pasceri, P., Stanford, W.L., et al. (2013). Modeling and rescue of the vascular phenotype of Williams-Beuren syndrome in patient induced pluripotent stem cells. Stem Cells Transl. Med. *2*, 2–15.

Lee, T.H., Song, S.H., Kim, K.L., Yi, J.Y., Shin, G.H., Kim, J.Y., Kim, J., Han, Y.M., Lee, S.H., Shim, S.H., et al. (2009). Functional recapitulation of smooth muscle cells via induced pluripotent stem cells from human aortic smooth muscle cells. Circ. Res. *106*, 120–128.

Michel, J.B., Li, Z., and Lacolley, P. (2012). Smooth muscle cells and vascular diseases. Cardiovasc. Res. *95*, 135–137.

Niklason, L.E., Gao, J., Abbott, W.M., Hirschi, K.K., Houser, S., Marini, R., and Langer, R. (1999). Functional arteries grown in vitro. Science *284*, 489–493.

Patsch, C., Challet-Meylan, L., Thoma, E.C., Urich, E., Heckel, T., O'Sullivan, J.F., Grainger, S.J., Kapp, F.G., Sun, L., Christensen, K., et al. (2015). Generation of vascular endothelial and smooth muscle cells from human pluripotent stem cells. Nat. Cell Biol. *17*, 994–1003.

Rubin, L.L. (2008). Stem cells and drug discovery: the beginning of a new era? Cell *132*, 549–552.

Sundaram, S., One, J., Siewert, J., Teodosescu, S., Zhao, L., Dimitrievska, S., Qian, H., Huang, A.H., and Niklason, L. (2014). Tissue-engineered vascular grafts created from human induced pluripotent stem cells. Stem Cells Transl. Med. *3*, 1535–1543.

Tavernier, G., Mlody, B., Demeester, J., Adjaye, J., and De Smedt, S.C. (2013). Current methods for inducing pluripotency in somatic cells. Adv. Mater. *25*, 2765–2771.

Wang, C., Cen, L., Yin, S., Liu, Q., Liu, W., Cao, Y., and Cui, L. (2010). A small diameter elastic blood vessel wall prepared under pulsatile conditions from polyglycolic acid mesh and smooth muscle cells differentiated from adipose-derived stem cells. Biomaterials *31*, 621–630.

Wang, Y., Hu, J., Jiao, J., Liu, Z., Zhou, Z., Zhao, C., Chang, L.J., Chen, Y.E., Ma, P.X., and Yang, B. (2014). Engineering vascular tissue with functional smooth muscle cells derived from human iPS cells and nanofibrous scaffolds. Biomaterials *35*, 8960–8969.

Wanjare, M., Kuo, F., and Gerecht, S. (2013). Derivation and maturation of synthetic and contractile vascular smooth muscle cells from human pluripotent stem cells. Cardiovasc. Res. *97*, 321–330.

Xie, C.Q., Zhang, J., Villacorta, L., Cui, T., Huang, H., and Chen, Y.E. (2007). A highly efficient method to differentiate smooth muscle cells from human embryonic stem cells. Arterioscler. Thromb. Vasc. Biol. *27*, e311–e312.

Zaragoza, C., Gomez-Guerrero, C., Martin-Ventura, J.L., Blanco-Colio, L., Lavin, B., Mallavia, B., Tarin, C., Mas, S., Ortiz, A., and Egido, J. (2011). Animal models of cardiovascular diseases. J. Biomed. Biotechnol. *2011*, 497841.

Zeiger, A.S., Loe, F.C., Li, R., Raghunath, M., and Van Vliet, K.J. (2012). Macromolecular crowding directs extracellular matrix organization and mesenchymal stem cell behavior. PLoS One *7*, e37904.

Stem Cell Reports, Volume *7*

Supplemental Information

Tissue-Engineered Vascular Rings from Human iPSC-Derived Smooth Muscle Cells

Biraja C. Dash, Karen Levi, Jonas Schwan, Jiesi Luo, Oscar Bartulos, Hongwei Wu, Caihong Qiu, Ting Yi, Yongming Ren, Stuart Campbell, Marsha W. Rolle, and Yibing Qyang

SUPPLEMENTAL FIGURES:

Figure S1. Related to Figure 1.

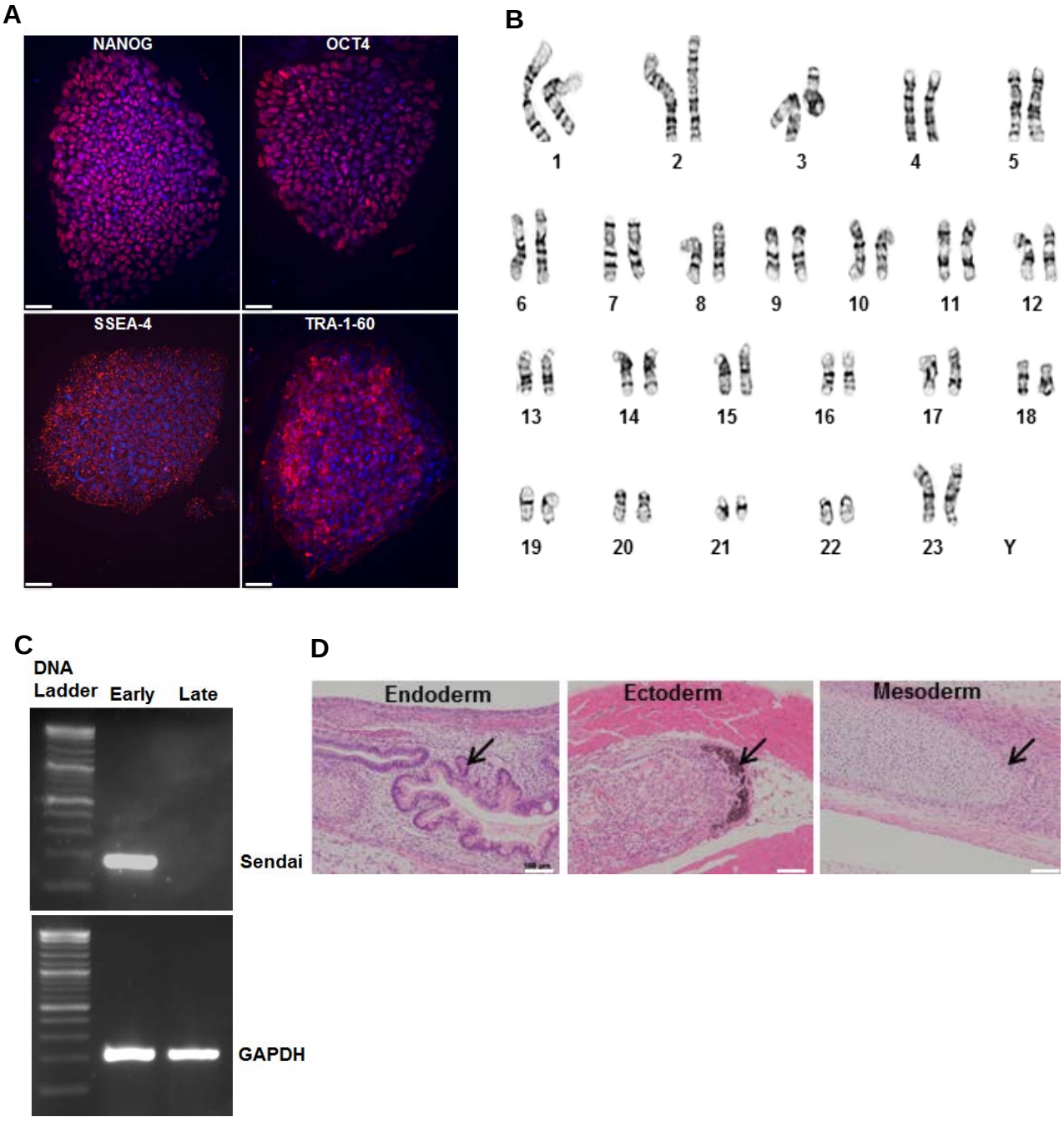

Figure S1. H**uman induced pluripotent stem cells (Y6) were generated using a Sendai virus vector and reprogramming factors OCT3/4, KLF4, c-MYC and SOX2.** (**A**) Human iPSC clones were selected and characterized for major pluripotency markers OCT4, SSEA4, NANOG, and Tra-1-60. Blue stains for nuclei, red stains for the pluripotency markers. Scale bar represents 100 µm. (**B**) G band staining for karyotype analysis of hiPSCs. (**C**) Detection of Sendai virus in the hiPSCs by RT-PCR analysis. GAPDH gene was used as the internal loading control.

Early passage hiPSCs (passage 2, “Early”; still containing virus) served as a positive control, while late passage hiPSCs (typically after passage 15, “Late”) lost the Sendai virus vector transgenes. (**D**) Teratoma formation after injection of undifferentiated hiPSCs in immunodeficient Rag2-/-GammaC-/- mice. Note the formation of gastrointestinal epithelium (endoderm, left), pigmented epithelium (ectoderm, center), and hyaline cartilage (mesoderm, right), as identified by the arrows. Scale bar represents 100 μm.

Figure S2. Related to Figure 1 and 2.

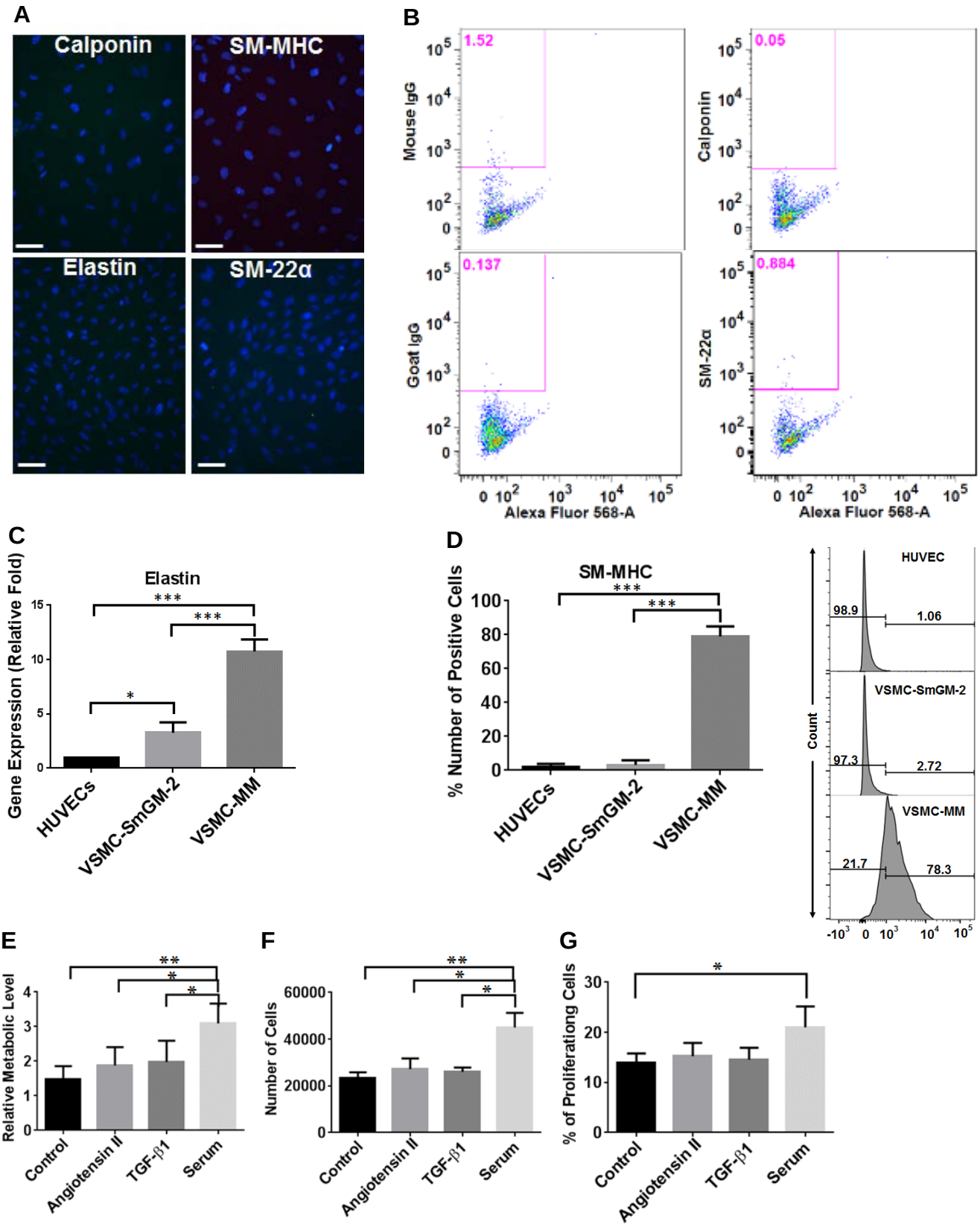

Figure S2: Analysis of hiPSC-VSMCs. (**A**) Immunofluorescence images of HUVECs stained for calponin, SM-22, elastin and SM-MHC. Blue stains for nuclei. Scale bar represents 50 µm. (**B**) FACS data showing HUVECs as a negative control for major smooth muscle cell specific markers SM-22 and calponin. Goat and mouse IgGs were used as experimental negative controls. Alexa Fluor 488 was used to gate positively stained cells. (**C**) qRT-PCR analysis of relative transcript amounts of elastin genes in hiPSC-VSMCs cultured in SmGM-2 and maturation (MM) medium (mean ± SD; n=3 independent experiments, *$p < 0.05$, ***$p<0.001$). HUVEC was used as a negative control. Values in the y-axis represent fold changes relative to human 18S expression. (**D**) Graph showing percentage of VSMCs positive for SM-MHC in three independent FACS experiments in SmGM-2 and maturation (MM) medium. HUVECs and rabbit IgG were used as negative and experimental control respectively (mean ± SD; n=3 independent experiments, ***$p<0.001$). Representative FACS plots showing SM-MHC quantification for HUVEC, VSMC-SmGM-2 and VSMC–MM. **(E-G)** Proliferative responses of hiPSC-VSMCs to different factors. Y6-VSMC proliferation was measured in response to control (chemically defined medium only), angiotensin II (10µM), TGF-β1 (5ng/ml), fetal bovine serum (10%) using (**E**) MTT assay (mean ± SD; n=4 independent experiments, *$p < 0.05$, **$p<0.01$), (**F**) cell counting (mean ± SD; n=3 independent experiments, *$p < 0.05$, **$p<0.01$) and (**G**) cell cycle analysis (mean ± SD; n=3 independent experiment, *$p < 0.05$) after 3 days in culture. Note that % of proliferating cells with cell cycle analysis (**G**) was quantified as the % of cells in S and G2-M phase. The data were represented as mean ± SD. Unpaired Student t-test was performed to determine statistical significance between control and treatment groups.

Figure S3. Related to Figure 1

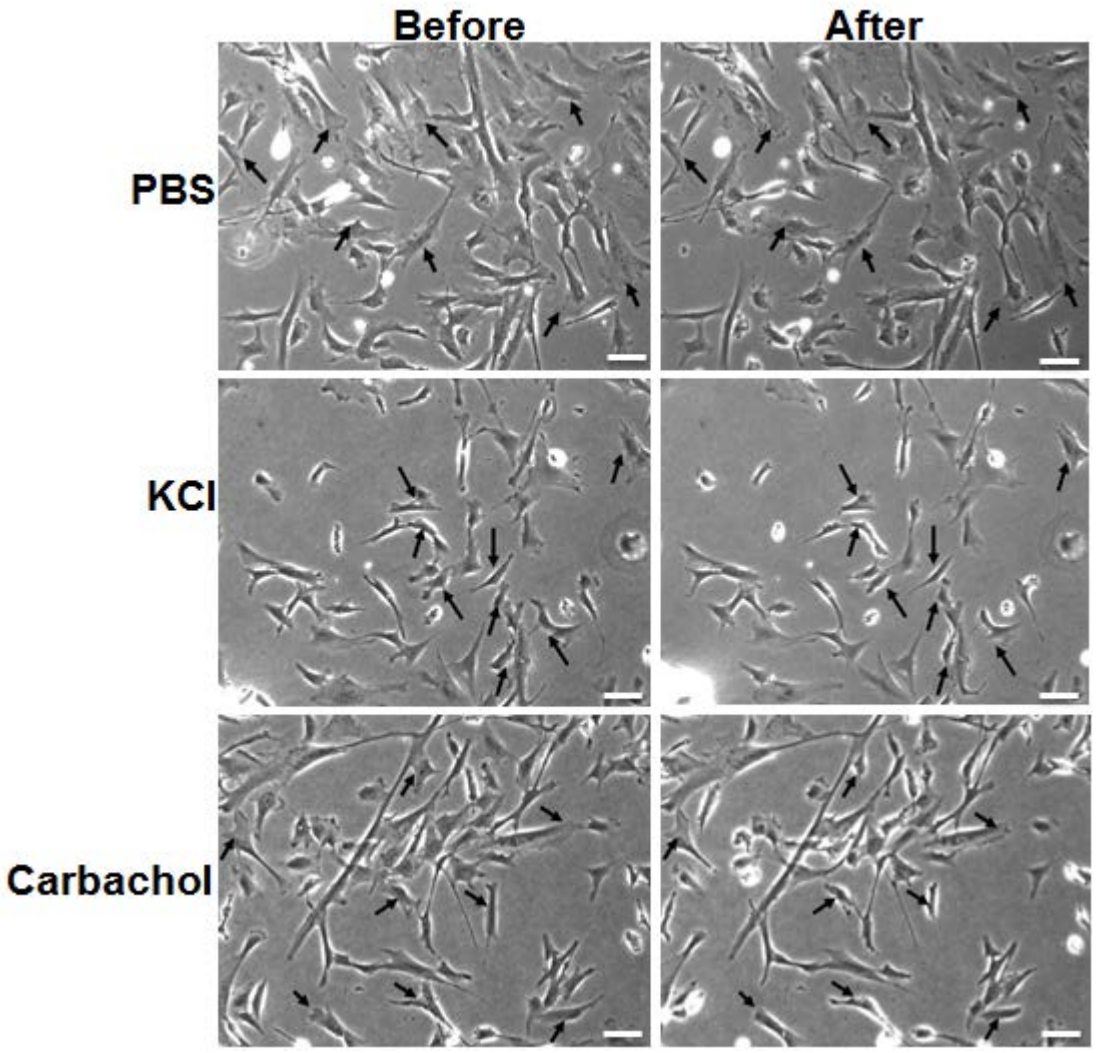

Figure S3: 2D Contractility response of VSMCs. Bright field images of Y6-VSMCs taken before and 15 minutes after adding agonists: KCl (50mM) and Carbachol (1mM). PBS was used as a negative control. Black arrows mark the cells quantified for decrease in the cell area. Scale bar represents 100 µm.

Figure S4. Related to Figure 3 and 4.

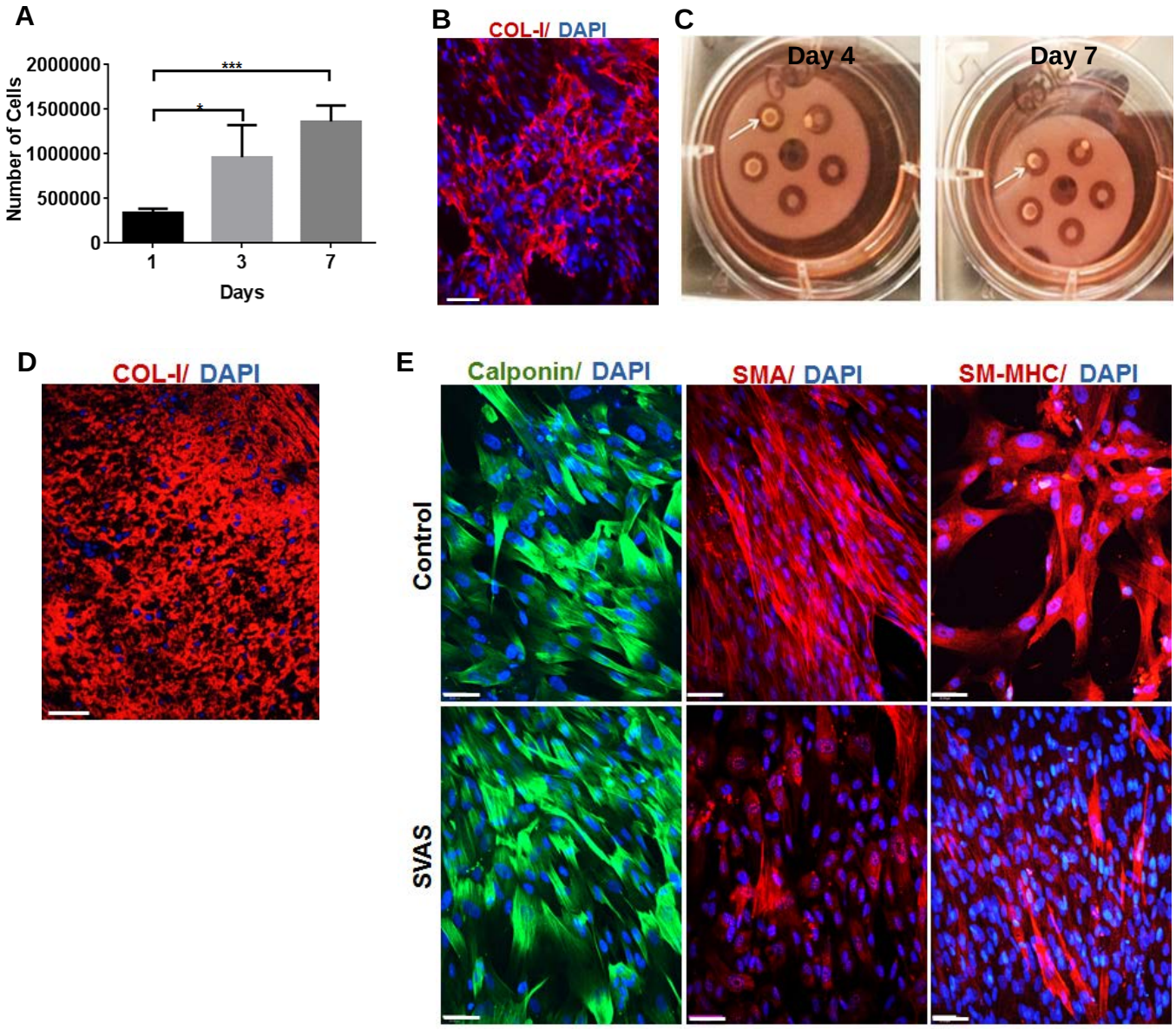

Figure S4. Tissue Ring and SVAS-VSMC characterization. (**A**) Proliferation of hiPSC-VSMCs in ring culture medium for day 1, 3 and 7 (mean ± SD; n=3 independent experiments,*p < 0.05, ***p < 0.001). (**B**) Immunofluorescence analysis of Y6-VSMCs cells producing type-I collagen in ring culture medium in a tissue culture plate within 7 days of culture. Collagen-1 (COL-1) stains red, and blue stains for nuclei). Scale bar represents 100 µm**. (C)** Photographs of Y6-VSMCs rings seeded in agarose wells cultured in SmGM-2 medium in a 6-well plate for 7 days. White arrows point to a typical tissue ring, which formed on day 4 (top panel) but was broken on day 7 (bottom panel). **(D)** Immunofluorescence analysis of Y6-VSMCs cells producing type-I collagen in the tissue ring after 14 days in culture. Collagen-1 (COL-1) stains red, and blue stains for nuclei). Scale bar represents 50 µm**. (E)** Analysis of control and SVAS iPSC-derived VSMCs in ring culture medium. Immunofluorescence images of cells stained with calponin and SMA and SM-MHC. Green stains for calponin and red for both SMA and SM-MHC. Blue stains

for nuclei. Scale bar represents 50 μm.

Table S1: Antibodies used in immunostaining

Antigen	catalog#	Isotype	Company
ES cell characterisation kit	SCR001	Mouse	EMD Millipore
α-SMA	Ab5694	Rabbit	Abcam
Calponin	C2687	Mouse	Sigma
SM-22α	Ab10135	Goat	Abcam
SM-MHC	Ab53219	Rabbit	Abcam
Collagen-I	Ab34710	Rabbit	Abcam
Elastin	Ab9519	Mouse	Abcam
Ki67	Ab15580	Rabbit	Abcam
Mouse IgG1 isotype control	MA1-10405	Mouse	Thermo Scientific
Goat IgG isotype control	02-6202	Goat	Thermo Scientific
Rabbit IgG isotype control	sc-2027	Rabbit	Santa Cruz Biotechnology
Alexa 488 goat anti-mouse IgG	A11029	N/A	Thermo Scientific
Alexa 555 goat anti-rabbit IgG	A21428	N/A	Thermo Scientific
Alexa 555 Donkey anti-goat IgG	A21432	N/A	Thermo Scientific

Table S2: List of primers used in qPCR assay.

human elastin F	AAGATGGTGCAGACACTTC
human elastin R	AGAGCGAATCCAGCTTTGG
human 18S F	GGAAGGGCACCACCAGGAGT
human 18S R	TGCAGCCCCGGACATCTAAG

EXPERIMENTAL PROCEDURES

Human iPSC Generation and Characterization

Fibroblasts were derived from discarded female neonatal skin tissue under Yale Institutional Review Board approval. The cells were plated at a density of 1×10^5 cells per well in a 6-well plate one day before transduction at approximately 60-70% confluence. CytoTune® Sendai tubes (3×10^6 CIU each; ThermoFisher, USA) were thoroughly mixed with 1 mL of pre-warmed fibroblast medium at 37°C. Then, culture medium was aspirated and replaced with 1 ml of the medium containing virus to each well. Twenty-four hours after transduction, the medium was replaced with fresh fibroblast medium. Seven days after transduction, fibroblast cells were harvested using 0.05% trypsin/EDTA and plated on a mitotically arrested mouse embryonic fibroblast (MEF) feeder layer. Twenty-four hours later, the MEF medium was replaced with iPSC medium (20% KSR in DMEM/F12 medium supplemented with 10ng/ml bFGF, 1% non-essential amino acid (v/v), and 2 mM L-Glutamine; all from ThermoFisher, USA). The medium was changed every day thereafter. Three weeks later, the iPSC colonies were manually picked and transferred onto Matrigel-coated plates and cultured in the mTeSR™1 medium (Stem Cell Technologies, USA) to expand the colonies (a clone named Y6 was used in this study). Total RNA was extracted from selected iPSC colonies from both early and late passage to determine the presence of Sendai RNA. RT-PCR analyses were performed to detect the expression of Sendai RNA using primers specific for its genomic DNA (Forward primer: GGATCACTAGGTGATATCGAGC; Reverse primer: ACCAGACAAGAGTTTAAGAGATATGTATC). GAPDH was used as the internal loading control (Forward primer: GAAGGTGAAGGTCGGAGTCA; Reverse primer: TTGAGGTCAATGAAGGGGTC). Passage 2 iPSC cultures were used as a positive control.

Pluripotency markers were analysed by immunofluorescence. Briefly, colonies of undifferentiated human iPSCs were fixed with 4% paraformaldehyde, permeabilized with 0.3% Triton X-100 and blocked with 5% fetal bovine serum. Specimens were incubated overnight at 4°C with primary antibodies for Tra-1-60, OCT4, NANOG and SSEA4 (EMD Millipore, USA), then incubated with secondary antibodies (1:1000 in PBS) for one hour at room temperature. DAPI (Life Technologies) was used to stain cell nuclei. The samples were examined using a fluorescent microscope. G-band staining for karyotype analysis was performed. Small clumps of human iPSC were seeded on glass slides pre-coated with Matrigel and fed with mTeSR™1 medium for three days. Then, medium was switched to DMEM basal medium supplemented with 10% of FBS (ThermoFisher, USA) for another 3 days. The slide was transferred to the Yale Cytogenetic Laboratory for G-band staining.

Teratoma formation was performed to assess iPSC pluripotency. Briefly, $1x10^6$ human iPSC cells were collected by collagenase treatment, and resuspended in 100 µl of DMEM/F12, collagen, and Matrigel mix (2:1:1 ratio). Cells were intramuscularly injected into immunodeficient Rag2-/-GammaC-/- mice. After 8 weeks, teratomas were harvested, fixed, and subjected to paraffin-embedding and hematoxylin and eosin (H/E) staining. All animal studies were approved by the Yale IACUC protocol (2013-11347) and performed in accordance with the NIH guidelines for care and use of laboratory animals.

Human iPSC-VSMC Derivation

Human iPSC-VSMCs were derived using an embryoid body (EB) method (Ge et al., 2012; Xie et al., 2007). Briefly, hiPSC lines including Y6 derived from healthy skin fibroblasts in this study; Control 1 derived from healthy VSMCs as describe previously (Ge et al., 2012) ; and Control 2 derived from healthy peripheral blood mononuclear cells as described previoiusly (Chen et al., 2013), were cultured under feeder-free conditions (mTeSR™1 medium) until they reached 80% confluency in a 6-well tissue culture plate (~4 days). hiPSC clumps of uniform sizes were harvested by cutting the colonies using a sharp glass tip and treating them with dispase (1mg/ml) for 15 min at 37 °C. To prepare EBs, hiPSC clumps were seeded in a 6-well low attachment plate with mTeSR™1 medium. The next day, the mTeSR™1 medium was replaced with a mixture of mTeSR™1 and EB differentiation medium (DMEM high glucose + 10% FBS + 1% non-essential amino acid (v/v) + 2mM L-glutamine and 0.012 mM 2-mercaptoethanol) in a ratio of 1 to 3. On day 3, the medium was replaced with EB differentiation medium. The EBs were cultured for the next 3 days in EB differentiation medium. By the end of day 5, the EBs were collected and seeded on a gelatin-coated 6-well plate for 5 days using EB differentiation medium. Medium was replaced with fresh EB medium every day. After the 5-day culture, the cells were harvested using 0.25% trypsin, seeded on Matrigel coated T75 flasks, and cultured until the VSMCs reached 80% confluence (~7 days). SmGM-2 medium (Lonza, USA) was used during the culture and was replaced with fresh medium every other day. Cells were subsequently cultured in either SmGM-2 (Lonza, USA), or a ring culture medium composed of Dulbecco's Modified Eagle Medium (DMEM; high glucose) with 20% FBS (Gibco® ThermoFisher, USA), PDGF-BB (10 ng/ml) (R&D Systems,

USA), TGF-β1 (1 ng/ml) (R&D Systems, USA), penicillin G (100U/ml) and supplemented with proline (50 µg/ml), glycine (50 µg/ml), alanine (20 µg/ml), $CuSO_4$ (3ng/ml) and ascorbic acid (50 µg/ml).

Immunofluorescence and Flow Cytometry

Human iPSC-VSMCs were characterized for smooth muscle cell protein expression by staining for smooth muscle α-actin (SMA), SM-22α, calponin, myosin heavy chain (SM-MHC) and elastin. Briefly, cells were fixed using 4% paraformaldehyde for 10 min, washed 3 times using PBS, and incubated with 10% goat serum or 5% bovine serum albumin (BSA) and 0.25% of Triton X-100 at 37 ºC for 1 hour. The cells were washed once with PBS and then incubated with 1:500 of polyclonal goat anti-SM-22α (Abcam, USA), 1:200 of monoclonal mouse anti-calponin (Sigma, USA), 1:100 of polyclonal rabbit anti-SM-MHC (Abcam, USA) and 1:100 of monoclonal mouse anti-elastin (Abcam, USA) in separate wells for overnight at 4 ºC. Alternatively, cells were stained with 1:200 polyclonal rabbit anti-collagen I primary antibody (Abcam, USA). After the primary antibody incubation, cells were washed with PBS/Tween-20 (PBST) three times for 5 minutes each wash. Finally, the cells were incubated with secondary antibodies (1:1000 in PBS): goat anti-mouse Alexa Fluor® 488 (ThermoFisher, USA), goat anti-rabbit Alexa Fluor® 568 (ThermoFisher, USA), or donkey anti-goat Alexa Fluor® 488 (ThermoFisher, USA) and DAPI (ThermoFisher, USA) for one hour. The cells were washed three times for 5 minutes each before fluorescence imaging.

For flow cytometry, harvested cells were fixed using 2% paraformaldehyde for 30 min at room temperature and washed with PBS three times followed by blocking with 5% BSA and 0.1% Triton-X-100. The primary antibodies SM-22α (Abcam, USA),calponin (Sigma, USA) and SM-MHC (Abcam, USA) were used in a final concentration of 1 µg/ml. Mouse,goat IgG and rabbit isotype controls (ThermoFisher, USA; Santa Cruz Biotechnology, USA) and non-expressing cell control (HUVECs) were used for both immunofluorescence and flow cytometry. Cell fluorescence was measured by a flow cytometer (BD, LSR II), and cell cycle analysis was done using FlowJo software. Refer to Table S1 for the catalog numbers for the antibodies used.

qRT-PCR Analysis

The HUVEC and human iPSC-derived VSMCs were subjected to RNA extraction and RT-PCR assay to evaluate the gene expression levels of elastin. RNA extraction and purification was completed by using the NucleoSpin RNA XS Total RNA Isolation Kit (Macherey-Nagle), following the manufacturer's instructions. Total RNA was then subjected to reverse transcription using an iScript cDNA synthesis Kit (Bio-rad). The primer sequences for the genes used in qPCR are listed in Table S2. qRT-PCR was performed using Bio-Rad IQ SYBR green supermix. The expression of elastin was normalized to that of human 18S.

VSMC Proliferation Assays

To determine the lineage of hiPSC-VSMCs, we measured cell proliferation in response to TGF-β1, angiotensin II and 10% FBS using MTT assay, cell counting and cell cycle analysis. For MTT assay, hiPSC-VSMCs were seeded 6,000 cells/well into 96-well plates using basal chemically defined medium (CDM) as previously described (Cheung et al., 2014; Cheung et al., 2012). Briefly, 500 ml of basal CDM contains 250 ml of IMDM, 250 ml of DMEM/F12, 5 ml of lipid concentrate, 1mg/ml of polyvinyl alcohol, 250 µl of transferrin, 350 µl of insulin and 20 µl of monothioglycerol. After incubation overnight, TGF-β1 (5 ng/ml, R&D System), angiotensin II (10 µM, Sigma) or 10% FBS (Gibco® ThermoFisher, USA) was added. Cell proliferation was measured as a function of the metabolic activity using MTT (Sigma) on different time points: Day 0 and 3. At every time point, MTT (0.5 mg/ml) was incubated with the cells at 37 °C for 2 h and then solubilized using DMSO (AmericanBIO, USA) at 37 °C for 15 min. Absorbance was measured at 540 nm using the Synergy 2 multi-mode plate reader (BioTek). To perform cell cycle analysis, hiPSC-VSMCs were harvested, and the cell suspension was fixed by ice cold 70% ethanol for 30 min at 4 °C followed by incubation with 100 µg/ml of RNase. Finally, cells were stained with 50 µg/ml of propidium iodide in the dark at 25 °C for 30 min. Cell fluorescence was measured by a flow cytometer (BD, LSR II), and cell cycle analysis was done using FlowJo software.

Tissue Ring Fabrication

Custom agarose molds for tissue ring formation were made as previously described, with minor modifications (Dikina et al., 2015; Gwyther et al., 2011a; Gwyther et al., 2011b). Briefly, a machined custom polycarbonate mold was created with 5 annular wells, each with posts 2 mm in diameter, designed to fit in one well of a 6-well plate. A polydimethylsiloxane (PDMS) mold was cured on the polycarbonate template, and was used to make wells from a 2% agarose solution in un-

supplemented DMEM (high glucose). The agarose molds were equilibrated in SmGM-2 medium overnight before rings were seeded. The hiPSC-VSMCs were harvested and seeded at 600,000 cells/well in SmGM-2. The rings were allowed to aggregate for 24 hours and were then cultured in ring culture medium composed of Dulbecco's Modified Eagle Medium (DMEM; high glucose) with 20% FBS (Gibco® ThermoFisher, USA), PDGF-BB (10 ng/ml) (R&D Systems, USA), TGF-β1 (1 ng/ml) (R&D Systems, USA), penicillin G (100U/ml) and supplemented with proline (50 µg/ml), glycine (50 µg/ml), alanine (20 µg/ml), $CuSO_4$ (3ng/ml) and ascorbic acid (50 µg/ml). The rings were harvested on either 14 or 17 days and analyzed by mechanical testing and histology.

2D and 3D Contractility Study

Two-dimensional (2D) SMC contraction studies were carried out using hiPSC-VSMCs cultured on tissue culture polystyrene. KCl (50mM) and carbachol (1mM) were used as agonists. Briefly, VSMCs were treated with agonists for 15 min, and images of pre- and post-treatments were acquired and decrease in the cell area was measured by ImageJ software.

For 3D contractility study, VSMC tissue ring was carefully removed from the culture and immersed in a temperature-controlled perfusion bath. The ring was picked up by two motorized micromanipulators with hook-like extensions, leaving the ring suspended between an anchoring attachment on one end and a force transducer (KG7, SI Heidelberg) on the other (see Figure 4C). Throughout measurements, the ring was incubated in Tyrode's solution (NaCl 140mM, KCl 5.4mM, MgCl2 1mM, HEPES 25mM, Glucose 10mM and 1.8mM $CaCl_2$, pH 7.3) freshly aerated with carbogen: 20% of oxygen,5% of carbon dioxide and 75% nitrogen. Force measurements were taken at the slack length before the manipulators were moved apart by a distance of 1.14 mm to take a second reference force measurement before agonist treatment. Either carbachol or KCl solutions were used in a final concentration of 1mM or 50mM respectively. The readings were taken for 15 min. Customized Matlab software was used to calculate the resulting changes in the force. For each ring, a baseline measurement was taken in PBS. Furthermore, cross sectional areas of the VSMC rings were acquired to calculate the changes in tension (Pa). The cross-section of the tissue rings were assessed using an optical coherence tomography (Ganymede-II-HR, Thorlabs). An index of refraction of 1.38 was used for each of the tissue rings. Four evenly distanced images were taken and their cross-sectional area were determined using Image J and averaged to give the overall cross sectional area of the tissue ring.

Tissue Ring Mechanical Testing

Before mechanical testing, the rings were removed from the posts and ring thickness measurements were taken as previously described (Gwyther et al., 2011a; Gwyther et al., 2011b). Briefly, four measurements were obtained at four different locations around the ring circumference using edge detection software (Framework, DVT), and were averaged to find the mean ring thickness. Mechanical testing was performed using a uniaxial tensile testing machine (Electropuls E1000, Instron) as previously described (Gwyther et al., 2011b). Briefly, rings were mounted on custom grips, loaded with a 5mN tare load, pre-cycled 8 times from 5mN to 50kPa, and pulled to failure at a rate of 10mm/min. Data were analyzed using a custom MATLAB program (The MathWorks Inc.) to calculate ultimate tensile strength (UTS) and maximum tangent modulus (MTM).

Histology and Immunohistochemistry

Tissue ring samples were paraffin-embedded and blocks were cut into sections of 5 µm thickness. Slides were stained with H/E and Masson's trichrome using standard protocols. VSMCs were identified by immunofluorescence staining of the VSMC specific markers calponin, SMA, SM-MHC, SM-22α and elastin using standard protocols (Refer to previous section). Briefly, tissue sections from the paraffin embedded samples were deparaffinized and processed through a gradient of alcohol from 100% to 50% ethanol and finally in water. Antigen retrieval was carried out at 100 ^{o}C using sodium citrate buffer (10mM sodium citrate, 0.05% Tween-20, pH 6.0). The primary and secondary antibodies were used as mentioned above in the immunofluorescence section. Slides were stained for type-I collagen using a similar protocol as above. The primary antibody used was polyclonal rabbit anti-type I collagen (1:200 in PBS containing 10% goat serum) and the secondary antibody was goat anti-rabbit Alexa Fluor® 568. Cell proliferation was measured between control and SVAS rings by staining slides with ki67 primary antibody (Abcam, USA; 1:200 in PBS containing 10% goat serum) and the goat anti-rabbit Alexa Fluor® 568 secondary antibody (1:1000 in PBS).

Statistical analysis

Statistical analyses were performed with GraphPad Prism 6. All the data were presented as mean ± SD. One-way ANOVA was used to compare the cell proliferation, elastin gene expression and SM-MHC FACS analysis, and unpaired Student t-test was used for comparisons.

REFERENCES:

Chen, I.P., Fukuda, K., Fusaki, N., Iida, A., Hasegawa, M., Lichtler, A., and Reichenberger, E.J. (2013). Induced pluripotent stem cell reprogramming by integration-free Sendai virus vectors from peripheral blood of patients with craniometaphyseal dysplasia. Cellular reprogramming *15*, 503-513.

Cheung, C., Bernardo, A.S., Pedersen, R.A., and Sinha, S. (2014). Directed differentiation of embryonic origin-specific vascular smooth muscle subtypes from human pluripotent stem cells. Nat Protoc *9*, 929-938.

Cheung, C., Bernardo, A.S., Trotter, M.W., Pedersen, R.A., and Sinha, S. (2012). Generation of human vascular smooth muscle subtypes provides insight into embryological origin-dependent disease susceptibility. Nat Biotechnol *30*, 165-173.

Dikina, A.D., Strobel, H.A., Lai, B.P., Rolle, M.W., and Alsberg, E. (2015). Engineered cartilaginous tubes for tracheal tissue replacement via self-assembly and fusion of human mesenchymal stem cell constructs. Biomaterials *52*, 452-462.

Ge, X., Ren, Y., Bartulos, O., Lee, M.Y., Yue, Z., Kim, K.Y., Li, W., Amos, P.J., Bozkulak, E.C., Iyer, A., *et al.* (2012). Modeling supravalvular aortic stenosis syndrome with human induced pluripotent stem cells. Circulation *126*, 1695-1704.

Gwyther, T.A., Hu, J.Z., Billiar, K.L., and Rolle, M.W. (2011a). Directed cellular self-assembly to fabricate cell-derived tissue rings for biomechanical analysis and tissue engineering. Journal of visualized experiments : JoVE, e3366.

Gwyther, T.A., Hu, J.Z., Christakis, A.G., Skorinko, J.K., Shaw, S.M., Billiar, K.L., and Rolle, M.W. (2011b). Engineered vascular tissue fabricated from aggregated smooth muscle cells. Cells Tissues Organs *194*, 13-24.

Xie, C.Q., Zhang, J., Villacorta, L., Cui, T., Huang, H., and Chen, Y.E. (2007). A highly efficient method to differentiate smooth muscle cells from human embryonic stem cells. Arterioscler Thromb Vasc Biol *27*, e311-312.